RSC Advances

PAPER

View Article Online
View Journal | View Issue

Cite this: *RSC Adv.*, 2021, **11**, 30873

Semi-synthetic puwainaphycin/minutissamide cyclic lipopeptides with improved antifungal activity and limited cytotoxicity†

Jan Hájek,‡[ab] Sebastian Bieringer,‡[cf] Kateřina Voráčová,[a] Markéta Macho,[ab] Kumar Saurav,[a] Kateřina Delawská,[ab] Petra Divoká,[a] Radovan Fišer,[d] Gabriela Mikušová,[d] José Cheel,[a] David P. Fewer,[e] Dai Long Vu,[a] Jindřiška Paichlová,[a] Herbert Riepl*[cf] and Pavel Hrouzek*[a]

Microbial cyclic lipopeptides are an important class of antifungal compounds with applications in pharmacology and biotechnology. However, the cytotoxicity of many cyclic lipopeptides limits their potential as antifungal drugs. Here we present a structure–activity relationship study on the puwainaphycin/minutissamide (PUW/MIN) family of cyclic lipopeptides isolated from cyanobacteria. PUWs/MINs with variable fatty acid chain lengths differed in the dynamic of their cytotoxic effect despite their similar IC_{50} after 48 hours (2.8 μM for MIN A and 3.2 μM for PUW F). Furthermore, they exhibited different antifungal potency with the lowest MIC values obtained for MIN A and PUW F against the facultative human pathogen *Aspergillus fumigatus* (37 μM) and the plant pathogen *Alternaria alternata* (0.6 μM), respectively. We used a Grignard-reaction with alkylmagnesium halides to lengthen the lipopeptide FA moiety as well as the Steglich esterification on the free hydroxyl substituents to prepare semi-synthetic lipopeptide variants possessing multiple fatty acid tails. Cyclic lipopeptides with extended and branched FA tails showed improved strain-specific antifungal activity against *A. fumigatus* (MIC = 0.5–3.8 μM) and *A. alternata* (MIC = 0.1–0.5 μM), but with partial retention of the cytotoxic effect (~10–20 μM). However, lipopeptides with esterified free hydroxyl groups possessed substantially higher antifungal potencies, especially against *A. alternata* (MIC = 0.2–0.6 μM), and greatly reduced or abolished cytotoxic activity (>20 μM). Our findings pave the way for a generation of semi-synthetic variants of lipopeptides with improved and selective antifungal activities.

Received 23rd June 2021
Accepted 2nd September 2021

DOI: 10.1039/d1ra04882a

rsc.li/rsc-advances

1. Introduction

Cyclic lipopeptides produced by a variety of bacteria and fungi have attracted attention as drug leads due to their potent antifungal, antibacterial, and cytotoxic properties.[1–3] Their structure is composed of a peptide cycle linked with a fatty acid (FA) moiety that may be part of the peptide backbone or attached as an exocyclic moiety.[1] The composition of the peptide cycle and the structure of the FA moiety affect the propensity of cyclic lipopeptides to interact with biological membranes and different types of cell walls.[4] A number of cyclic lipopeptides contain positively charged amino acid residues, which promote interaction with negatively charged bacterial cell walls and membranes.[1,5] Antibacterial cyclic lipopeptides include polymyxins and daptomycin, which are approved for topical application or parenteral administration as treatment for various bacterial infections.[1] Cyclic lipopeptides containing neutral amino acid residues exhibit a range of bioactivities, including cytotoxicity against human cells as well as antifungal bioactivity.[1,6] The majority of known antifungal cyclic lipopeptides are produced by bacteria (*e.g.* iturins, surfactin, and fengycin) and form organized aggregates in biological membranes, which cause early membrane damage through ion leakage that subsequently leads to membrane disintegration.[6–8] However, in some cases the antifungal effect is achieved through enzyme inhibition rather than membrane damage, *e.g.* caspofungin exerts antifungal activity through selective inhibition of β-D-glucan synthase.[9]

[a]*Centre Algatech, Institute of Microbiology of the Czech Academy of Sciences, Opatovický mlýn, Novohradská 237, 379 81 Třeboň, Czech Republic. E-mail: hrouzek@alga.cz*

[b]*Faculty of Science, University of South Bohemia in České Budějovice, Branišovská 1760, 37005, České Budějovice, Czech Republic*

[c]*TUM Campus Straubing for Biotechnology and Sustainability, Technical University Munich, 94315 Straubing, Germany. E-mail: herbert.riepl@hswt.de*

[d]*Faculty of Science, Charles University, Viničná 5, 128 44 Prague 2, Czech Republic*

[e]*Department of Microbiology, University of Helsinki, Biocenter 1, Viikinkaari 9, FIN-00014 Helsinki, Finland*

[f]*Weihenstephan-Triesdorf University of Applied Sciences, Organic-analytical Chemistry, 94315 Straubing, Germany*

† Electronic supplementary information (ESI) available. See DOI: 10.1039/d1ra04882a

‡ These authors contributed equally.

Structure–activity relationship analysis (SAR) has been used extensively to study members of the iturin family,[6] which manifest significant antifungal activity (MIC values of 1.25–5 μM) against a broad range of fungi.[6,10–12] Their potency has been found to be substantially affected by both the amino-acid composition of the cyclic peptide as well as variation in the FA moiety length.[6] Members of the iturin family have a seven-membered ring containing an invariable Tyr residue, which is essential for compound folding[6] with *O*-methylation of Tyr reducing the potency of iturin.[13] The absence of a FA tail entirely abolishes the antifungal effect as demonstrated in bioassays using synthetic variants lacking FA moiety.[6] Natural variants bearing longer FA tails manifest stronger antifungal and haemolytic activity compared to those with shorter FA tails.[6] However, the effect of FA residue length on the bioactivity of cyclic lipopeptides has received only limited attention,[14] despite the large variation in FA tail length reported for the majority of antifungal cyclic lipopeptides.[15,16]

The structural diversity of cyclic lipopeptides found in cyanobacteria is similar to that found in other bacterial lineages.[17–23] Several classes of cyclic cyanobacterial lipopeptides are reported to possess potent antifungal potency,[24] namely hassallidins,[25] laxaphycins,[26] muscotoxins,[19,27] anabaenolysins,[28] puwainaphycins,[20,29] and minutissamides.[16,18] However, these lipopeptides also display prominent cytotoxic activity and/or haemolytic activity *in vitro*, which strongly contradicts use in human or veterinary medicine.

The puwainaphycin/minutissamide (PUWs/MINs) family of cyclic lipopeptides with incorporated β-amino-α-hydroxy-γ-methyl FA moiety exhibits structural similarities to members of the iturin family (Fig. 1).[17,18,20,29] A hybrid biosynthetic pathway combining enzymes of non-ribosomal peptide synthetases (NRPS) and polyketide synthase (PKS) is responsible for their biosynthesis. This pathway employs alternative starter modules containing fatty-acyl AMP-ligases capable of incorporating FAs with a variable chain length and accessory enzymes that can further modify the FA residue.[16,30] This biosynthetic machinery generates the wide structural variability of PUWs/MINs that includes variants bearing FA moiety consisting of C10-18 (ref. 15) that may be further functionalized with oxo-, hydroxy-, and chloro-substituents.[16] PUWs/MINs exhibit moderate cytotoxic effects in human cells connected to membrane damage resulting in necrotic cell death.[20] In addition, PUWs/MINs exhibit antifungal potency against *Saccharomyces cerevisiae* and *Candida albicans*.[16] Previous findings have suggested that the length of the FA residue may affect antifungal activity.[16] Despite structural variability, it is notable that the FA residue of PUW/MIN chemical variants contain both a conserved β-amino-α-hydroxy-γ-methyl motif and amino acids adjacent to the FA residue, suggesting that these residues are important for the resulting bioactivity.

Cyanobacterial cyclic lipopeptides have not previously been the subject of SAR studies or chemical improvement of their bioactivity properties. In the present study, we have performed a SAR study on the PUW/MIN group of cyclic lipopeptides in order to uncover the effect of FA moiety length on both antifungal and cytotoxic activity.

2. Experimental section

Cultivation of cyanobacterial biomass and extraction

The cyanobacterial strains *Cylindrospermum alatosporum* CCALA 988 and *Anabaena* sp. UHCC-0399 were cultivated in multiple 350 mL glass tubes in liquid BG-11 and bubbled with 1.5% CO_2-enriched air at a constant temperature of 28 °C under 50 W m^{-2} continuous illumination. After reaching the late

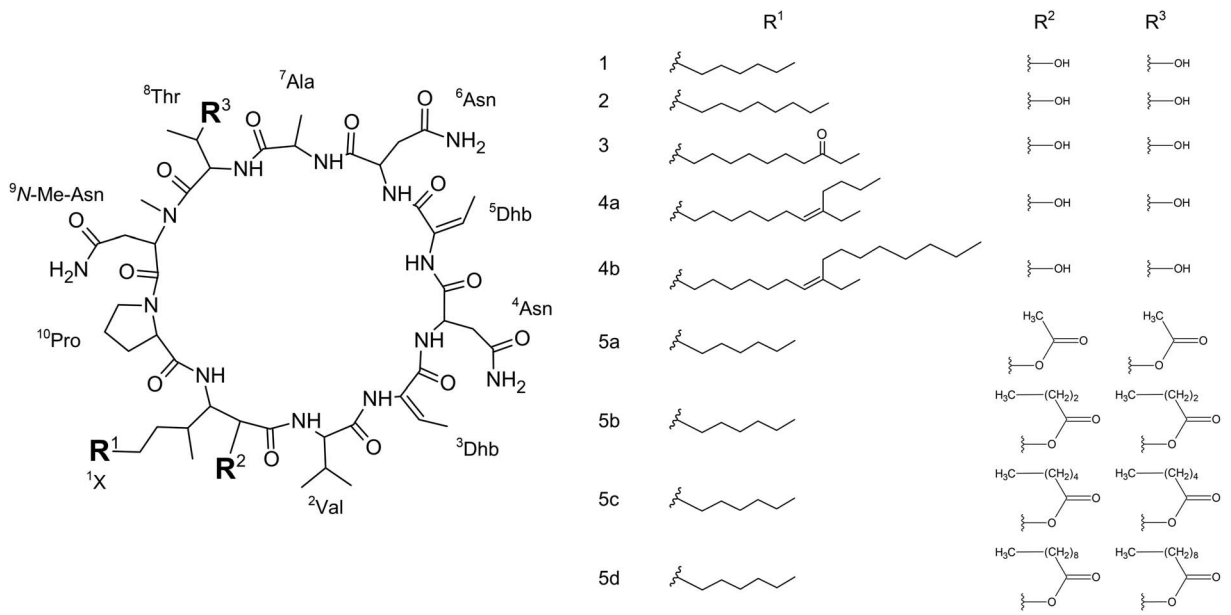

Fig. 1 Naturally occurring and semi-synthetic PUW/MIN variants. Compounds **1** (MIN A), **2** (PUW F), and **3** (MIN C) were isolated from cyanobacteria. Compounds **4a–5d** are semi-synthetic analogs prepared within this study.

exponential phase the culture was transferred consecutively to 15 L and 100 L photobioreactors set to control identical temperature and illumination conditions. The culture was harvested by centrifugation after 10–14 days of cultivation and freeze-dried (Leybold-Heraeus freeze-drier Lyovac GT 3). 10 g of lyophilized biomass was extracted using MeOH/H_2O (70/30, v/v) for 1 hour and centrifuged at 4500 rpm. The supernatant was collected and evaporated using a rotary evaporator until dryness while temperature did not exceed 40 °C. The residue was dissolved in 5 mL of acidified MeOH.

HPLC purification of PUW F, MIN A and MIN C

PUW F and MIN A were isolated from *Cylindrospermum alatosporum* CCLA 988 using previously optimized protocols.[31] MIN C was isolated from biomass of *Anabaena* sp. UHCC-0399. Methanol extract solution (acidified by 0.1% v/v HCOOH) was purified on an HPLC Agilent 1260 infinity series chromatograph equipped with preparative pumps, a multi-wavelength detector, and an automatic fraction collector. A preparative Reprosil RP-C18 column (5 μm; 25 × 250 mm) with MeOH + 0.1% HCOOH (A)/10% MeOH aq. + 0.1% HCOOH (B) gradient at a flow rate of 10 mL min^{-1} was eluted using the following gradient: 0 min – 0% of A; 6 min – 0% of A; 15 min – 57% of A; 43 min – 76% of A; 45 min – 100% of A; 52 min – 100% of A; 60 min – 0% of (A). Fractions were collected using an automatic fraction collector at 1 min intervals and were checked for compound content using HPLC-HRMS/MS analysis. Fractions containing the desired PUW/MIN variants were evaporated on a rotary vacuum evaporator and resuspended in 1 mL of MeOH. The second purification step was performed using an Agilent 1100 Series modular HPLC system (Agilent Technologies 1100 Series) equipped with a diode array detector on semi-preparative Agilent Eclipse XDB-C18 column (5 μm; 9.4 × 250 mm) and ACN + 0.1% HCOOH (A)/H_2O + 0.1% HCOOH (B) gradient at a flow-rate of 2 mL min^{-1} (0 min – 30% of A; 2 min – 30% of A; 6 min – 42% of A; 15 min – 55% of A; 16 min – 100% of A; 20 min 100% of A; 21 min 30% of A). Fractions containing MIN C (collected at retention time range 8–12 min.) were collected manually using a UV detection set to 235 nm, evaporated on rotary evaporator and resuspended again in 1 mL of MeOH.

Chemical synthesis

General considerations. If not otherwise stated, reactions were performed in an argon atmosphere with dry solvents. All reagents and solvents were purchased from VWR, Sigma-Aldrich, Alfa Aesar, Acros Organics, and Abcr. The obtained products were purified by reversed phase HPLC on a Luna 250 × 15 mm Column (Phenomenex) with a Puriflash 4250–250 from Interchim. NMR-spectra were recorded on a JEOL ECS-400 (400 MHz) Nuclear Magnetic Resonance (NMR) spectrometer. Chemical shifts were reported in ppm and are referenced to residual protons in the deuterated solvent as the internal standard.

General procedure for the extension of the FA chain in MIN C

MIN C (50 mg, 0.042 mmol, 1 eq.) was dissolved in a flame-dried round bottom flask in dry THF (20 mL) under argon atmosphere. Two mL of a Grignard solution was added dropwise *via* syringe through a septum cap at 0 °C under stirring. The reaction was mixed by stirring at 0 °C for a further 5 min and then allowed to warm up to room temperature. The reaction was quenched after 2 h with 15 mL of aq. NH_4Cl. THF was removed *in vacuo* at 32 °C. The resulting mixture was loaded on a SPE-column packed with 40 g C18 silica and eluted with 30 mL of H_2O, 2 : 8 ACN/H_2O and 9 : 1 ACN/H_2O. Products were found in the 9 : 1 H_2O/ACN fraction. The products were used in the following steps with no further purification after removal of the volatiles under reduced pressure.

The material was dissolved in dry $CHCl_3$ (20 mL) in a flame-dried round-bottom flask under N_2 atmosphere. Subsequently, *p*-TsOH (45 mg, 0.29 mmol) was added under a constant flow of nitrogen. The reaction was mixed by stirring for 2 h at 35 °C. The reaction was quenched with H_2O (15 mL) and chloroform was removed under reduced pressure at 32 °C. The resulting mixture was loaded on a SPE-column packed with 40 g C18 silica and eluted with 30 mL of H_2O, 2 : 8 ACN/H_2O, and 9 : 1 ACN/H_2O. Products were found in the 9 : 1 ACN/H_2O fraction. The products were purified further by reversed phase HPLC (40 : 60 to 95 : 5 MeOH/H_2O, Luna 250 × 15 mm, C18 silica) following removal of the volatiles under reduced pressure.

Compound 4a. MIN C was converted with butylmagnesium chloride (1.5 M in THF/Toluene, 36 eq.) to give the title compound as white solid. Yield: 1.2 mg (0.001 mmol, 2%). Purity: 93.17% (UV/VIS base peak purity, 205–800 nm, $\int_{\mathbf{4a}} = 341$, $\int_{\text{contaminants}} = 25$). HRMS: $[M + 2H^+]^{2+}$ 614.8684, calcd 614.8692 for $[C_{59}H_{97}N_{13}O_{15} + 2H^+]^{2+}$. ^{1}H NMR (400 MHz, CD_3OD) δ 7.30 (d, $J = 9.2$ Hz, 1H), 6.86 (d, $J = 8.7$ Hz, 1H), 5.91 (d, $J = 7.6$ Hz, 1H), 5.52 (d, $J = 7.6$ Hz, 1H), 5.36 (s, 2H), 4.59 (s, 1H), 4.46 (d, $J =$ 15.3 Hz, 1H), 4.30 (d, $J = 6.0$ Hz, 1H), 4.14 (s, 2H), 3.84 (s, 2H), 3.67–3.61 (m, 9H), 3.50–3.48 (m, 1H), 3.14 (dt, $J = 3.2$, 1.8 Hz, 1H), 3.06 (s, 1H), 2.17 (t, $J = 7.6$ Hz, 4H), 1.99 (d, $J = 7.8$ Hz, 3H), 1.79 (d, $J = 7.8$ Hz, 2H), 1.60 (s, 5H), 1.44–1.28 (m, 50H), 1.13 (d, $J = 6.4$ Hz, 2H), 1.03 (d, $J = 6.9$ Hz, 2H), 0.95–0.88 (m, 9H), 0.76 (d, $J = 6.9$ Hz, 1H), 0.72 (s, 3H).

Compound 4b. MIN C was converted with octylmagnesium bromide (2 M in THF, 48 eq.) to give the title compound as white solid. Yield: 0.7 mg (0.5 μmol, 1%). Purity: 94.95% (UV/VIS purity, 205–800 nm, $\int_{\mathbf{4b}} = 46\,944$, $\int_{\text{cont.}} = 2499$). HRMS: $[M + 2H^+]^{2+}$ 642.8986, calcd 642.9005 for $[C_{63}H_{105}N_{13}O_{15} + 2H^+]^{2+}$. ^{1}H NMR (400 MHz, CD_3OD) δ 8.64 (s, 1H), 7.72 (d, $J = 8.9$ Hz, 1H), 7.24 (d, $J = 10.5$ Hz, 1H), 5.89 (d, $J = 7.3$ Hz, 1H), 5.70 (d, $J =$ 8.9 Hz, 1H), 5.51 (d, $J = 7.4$ Hz, 1H), 4.55 (d, $J = 16.8$ Hz, 2H), 4.45–4.41 (m, 2H), 4.28 (d, $J = 6.5$ Hz, 1H), 4.22 (s, 1H), 4.09 (s, 2H), 3.04 (s, 3H), 2.76–2.59 (m, 3H), 2.16 (s, 1H), 2.13 (s, 1H), 1.99 (dd, $J = 15.2$, 7.4 Hz, 9H), 1.77 (d, $J = 7.5$ Hz, 3H), 1.56 (d, J $= 6.8$ Hz, 3H), 1.37 (d, $J = 55.1$ Hz, 42H), 1.11 (d, $J = 6.4$ Hz, 3H), 1.01 (d, $J = 6.8$ Hz, 3H), 0.96–0.87 (m, 10H), 0.74 (d, $J = 6.6$ Hz, 3H).

General procedure for the esterification of free hydroxyl groups in MIN A

MIN A (20 mg, 0.018 mmol, 1 eq.) was dissolved in 15 mL dry ACN in a flame-dried round-bottomed flask under argon

atmosphere. DMAP (240 mg, 2.13 mmol, 109 eq.) was added under a constant flow of argon. The respective carboxylic anhydride (0.54 mmol, 30 eq.) was added dropwise *via* syringe through a septum cap. The reaction was mixed by stirring for 20 h at room temperature and then quenched with H_2O. The mixture was loaded on a SPE-column packed with 40 g C18 silica after removal of ACN *in vacuo* at 32 °C and eluted with 30 mL of H_2O, 2 : 8 ACN/H_2O, and 9 : 1 ACN/H_2O. Products were found in the 1 : 9 H_2O/ACN fraction. The products were further purified by reversed phase HPLC (40 : 60 to 95 : 5 MeOH/H_2O, Luna 250 × 15 mm, C18 silica) after removal of the volatiles under reduced pressure.

Compound 5a. MIN A was converted according to the general procedure with 57 μL acetic anhydride to give the title compound as white solid. Yield: 2.6 mg (0.002 mmol, 12%). Purity: 95.96% (UV/VIS purity, 205–800 nm, $\int_{\mathbf{5a}} = 2\,469\,933$, $\int_{\text{cont.}} = 103\,924$). HRMS: 1202.6405 $[M + H]^+$, calcd 1202.6421 for $[C_{55}H_{87}N_{13}O_{17} + H^+]^+$. ^{1}H NMR (400 MHz, CD_3OD) δ 7.72 (d, J = 8.2 Hz, 1H), 7.58 (d, J = 10.2 Hz, 1H), 6.59 (d, J = 7.3 Hz, 1H), 5.91 (q, J = 7.6 Hz, 1H), 5.67 (d, J = 12.6 Hz, 1H), 5.53 (d, J = 7.4 Hz, 1H), 5.48 (d, J = 4.8 Hz, 1H), 5.38–5.03 (m, 4H), 4.69–4.43 (m, 3H), 4.34–4.15 (m, 3H), 3.20–2.72 (m, 9H), 2.65 (s, 10H), 2.21 (d, J = 15.2 Hz, 3H), 2.09 (d, J = 2.1 Hz, 3H), 2.06–1.92 (m, 7H), 1.83 (d, J = 7.2 Hz, 2H), 1.75 (d, J = 7.5 Hz, 3H), 1.47–1.22 (m, 18H), 1.18 (d, J = 6.4 Hz, 3H), 1.00 (d, J = 6.8 Hz, 3H), 0.89 (d, J = 8.0 Hz, 6H), 0.72 (d, J = 6.7 Hz, 3H).

Compound 5b. MIN A was converted according to the general procedure with 110 μL butanoic anhydride to give the title compound as white solid. Yield: 10 mg (0.008 mmol, 44%). Purity: 93.48% (UV/VIS purity, 205–800 nm, $\int_{\mathbf{5b}} = 731\,946$, $\int_{\text{cont.}} = 51\,022$). HRMS: 1258.7102 $[M + H]^+$, calcd 1258.7047 for $[C_{59}H_{95}N_{13}O_{17} + H^+]^+$. ^{1}H NMR (400 MHz, CD_3OD) δ 5.91 (q, J = 7.3 Hz, 1H), 5.69 (dd, J = 12.0, 3.2 Hz, 1H), 5.54 (d, J = 7.5 Hz, 1H), 5.50 (d, J = 4.7 Hz, 1H), 5.25 (t, J = 6.2 Hz, 1H), 5.06 (dd, J = 9.7, 5.6 Hz, 2H), 4.63 (dd, J = 8.3, 3.4 Hz, 1H), 4.54 (d, J = 7.3 Hz, 1H), 4.50–4.46 (m, 1H), 4.29 (d, J = 7.2 Hz, 1H), 4.21 (dd, J = 11.3, 4.7 Hz, 1H), 3.35 (s, 3H), 3.19 (s, 3H), 3.08–2.76 (m, 6H), 2.36 (td, J = 7.3, 1.8 Hz, 2H), 2.27–2.18 (m, 4H), 1.99 (d, J = 7.4 Hz, 3H), 1.76 (d, J = 7.4 Hz, 3H), 1.71–1.65 (m, 3H), 1.60–1.52 (m, 2H), 1.41–1.28 (m, 20H), 1.19 (d, J = 6.4 Hz, 3H), 1.02–0.86 (m, 21H), 0.73 (d, J = 6.5 Hz, 3H). ^{13}C NMR (101 MHz, CD_3OD) δ 174.90, 174.78, 174.39, 173.79, 173.00, 172.51, 171.08, 170.64, 169.91, 168.24, 165.49, 165.38, 133.12, 129.67, 120.38, 73.12, 70.73, 61.48, 58.24, 55.82, 54.49, 51.94, 50.94, 50.18, 40.43, 36.88, 36.66, 35.10, 34.40, 33.89, 32.85, 31.06, 30.56, 30.21, 26.40, 24.91, 23.53, 19.45, 19.12, 19.09, 18.49, 17.31, 16.75, 16.10, 14.22, 13.82, 13.72, 13.59, 13.50.

Compound 5c. MIN A was converted according to the general procedure with 130 μL hexanoic anhydride to give the title compound as white solid. Yield: 13 mg (0.01 mmol, 55%). Purity: 94.67% (UV/VIS purity, 205–800 nm, $\int_{\mathbf{5c}} = 1\,088\,096$, $\int_{\text{cont.}} = 61\,248$). HRMS: 1314.7674 $[M + H]^+$, calcd 1314.7673 for $[C_{63}H_{103}N_{13}O_{17} + H^+]^+$. ^{1}H NMR (400 MHz, CD_3OD) δ 5.91 (q, J = 7.4 Hz, 1H), 5.69 (dd, J = 12.4, 3.2 Hz, 1H), 5.58–5.48 (m, 2H), 5.29–5.21 (m, 1H), 5.11–5.02 (m, 2H), 4.64 (dd, J = 8.4, 3.4 Hz, 1H), 4.54 (q, J = 7.3 Hz, 1H), 4.51–4.47 (m, 1H), 4.37–4.27 (m, 2H), 4.21 (dd, J = 11.3, 4.7 Hz, 1H), 3.43–3.33 (m, 1H), 3.19 (s, 3H), 3.10–2.74 (m, 6H), 2.37 (t, J = 7.5 Hz, 2H), 2.30–2.00 (m, 7H), 1.99 (d, J = 7.4 Hz, 3H), 1.96–1.86 (m, 2H), 1.83 (t, J = 6.9 Hz, 2H), 1.75 (d, J = 7.5 Hz, 3H), 1.71–1.48 (m, 5H), 1.48–1.24 (m, 30H), 1.19 (d, J = 6.4 Hz, 3H), 1.00 (d, J = 6.8 Hz, 3H), 0.97–0.85 (m, 15H), 0.73 (d, J = 6.7 Hz, 3H). ^{13}C NMR (101 MHz, CD_3OD) δ 175.11, 175.00, 174.86, 174.62, 174.01, 173.18, 172.97, 172.72, 171.25, 170.85, 170.11, 168.43, 165.69, 165.57, 133.33, 130.14, 129.79, 120.58, 73.36, 70.89, 61.68, 58.45, 56.01, 54.67, 52.58, 51.17, 50.43, 40.70, 39.17, 37.13, 35.32, 35.14, 34.98, 34.60, 34.12, 33.06, 32.44, 32.34, 31.63, 31.26, 30.77, 30.41, 26.58, 25.61, 25.57, 25.17, 23.74, 23.43, 23.38, 19.66, 18.76, 17.52, 16.98, 16.32, 14.44, 14.28, 14.25, 13.82, 13.72.

Compound 5d. MIN A was converted according to the general procedure with 176 μL decanoic anhydride to give the title compound as white solid. Yield: 6 mg (0.004 mmol, 23%). Purity: 96.10% (UV/VIS purity, 205–800 nm, $\int_{\mathbf{5d}} = 556\,092$, $\int_{\text{cont.}} = 22\,574$). HRMS: 713.9501 $[M + 2H]^{2+}$, calcd 713.9502 for $[C_{71}H_{119}N_{13}O_{17} + H^{2+}]^{2+}$. ^{1}H NMR (400 MHz, CD_3OD) δ 7.57 (d, J = 10.1 Hz, 1H), 5.91 (q, J = 7.3 Hz, 1H), 5.69 (d, J = 10.1 Hz, 1H), 5.55 (t, J = 7.3 Hz, 1H), 5.50 (t, J = 5.0 Hz, 1H), 5.29–5.20 (m, 1H), 5.09–5.02 (m, 2H), 4.64 (dd, J = 8.5, 3.4 Hz, 1H), 4.61–4.45 (m, 3H), 4.36–4.17 (m, 4H), 3.19 (s, 3H), 3.04–2.80 (m, 4H), 2.37 (t, J = 7.4 Hz, 3H), 2.33–2.19 (m, 5H), 1.99 (d, J = 7.4 Hz, 4H), 1.75 (d, J = 7.4 Hz, 6H), 1.65 (t, J = 7.4 Hz, 3H), 1.41–1.26 (m, 58H), 1.19 (d, J = 6.4 Hz, 3H), 1.00 (d, J = 6.9 Hz, 3H), 0.90 (dt, J = 7.3, 3.6 Hz, 17H), 0.73 (d, J = 6.8 Hz, 3H). ^{13}C NMR (101 MHz, CD_3OD) δ 174.80, 174.41, 173.81, 172.97, 172.74, 171.04, 169.90, 168.23, 165.47, 133.10, 129.94, 120.37, 70.65, 61.48, 58.25, 54.47, 50.98, 50.02, 40.56, 34.99, 34.82, 34.40, 33.93, 32.83, 31.07, 30.56, 30.37, 30.33, 30.28, 30.21, 30.05, 29.96, 26.36, 25.73, 25.66, 24.66, 23.53, 19.46, 18.59, 17.31, 16.80, 16.11, 14.24, 13.60, 13.50.

Purification of semi-synthetic variants

Fine purification of semi-synthetic PUW/MIN variants was performed on an Agilent 1100 Series modular HPLC system (Agilent Technologies) equipped with a MWD using a semi-preparative RP-C18 column with ACN + 0.1% HCOOH (A)/H_2O + 0.1% HCOOH (B) gradient at a flow-rate of 2.5 mL min^{-1} (0 min – 50% of A; 1 min – 50% of A; 25 min – 95% of A; 26 min – 100% of A; 36 min – 100% of A; 37 min – 50% of A). Fractions were collected manually using UV detection at 215, 235, 280, 440, and 680 nm, while 235 nm was mainly used due to the high absorption of both lipopeptides and possible contaminants at this wavelength. Because of the low ionizability of modified variants, the purity was determined based on the integration of the compound peak area in UV/VIS 205–800 nm chromatograms. In the case of **5a–d**, both lipopeptide isomers were taken together, in the case of **4a**, due to its low concentration, a UV/VIS base peak chromatogram was used.

HPLC-HRMS and HRMS/MS analysis

The purity of natural PUW/MIN as well as their semi-synthetic variants was monitored by HPLC-HRMS on Thermo Scientific Dionex UltiMate 3000 UHPLC+ (Sunnyvale, CA, USA) equipped with a diode-array detector. Separation of compounds was

performed on reversed phase Phenomenex Kinetex C18 column (150 × 4.6 mm, 2.6 μm, Torrance, CA, USA) using H_2O (A)/ACN (B) both containing 0.1% HCOOH as a mobile phase with the flow rate of 0.5 mL min^{-1}. The gradient was as follows: A/B 85/15 (0 min), 85/15 (in 1 min), 0/100 (in 39 min), 0/100 (in 44 min), and 85/15 (in 49 min). The HPLC was connected to Bruker Impact HD high-resolution mass spectrometer (Bruker, Billerica Massachusetts, USA) with electrospray ionization. The following settings were used: dry temperature 200 °C; drying gas flow 12 L min^{-1}; nebulizer 3 bar; capillary voltage 4500 V; endplate offset 500 V. The MS/MS experiments were performed with identical instrument settings to confirm the chemical structure of the synthetized PUWs/MINs. Collision energy of 80 eV for single charged and 35 eV double charged ions was used. The spectra were collected in the range of 20–2000 *m*/*z* with a spectra rate of 3 Hz. Spectra were calibrated using both LockMass Tuning Mix ES-TOF (622 Da) internal calibration solution and sodium formate clusters at the beginning of each analysis.

Cytotoxicity testing using MTT and recovery experiments

Lipopeptide cytotoxicity was tested on a human cervical cancer cell line (HeLa cells) cultured in RPMI 1640 medium (supplemented with 10% FBS, 2 mM L-glutamine and 1% antibiotics). The cells were incubated at 37 °C and 5% CO_2 in humidified incubator. For dose–response curves, 10×10^3 cells per well (200 μL) were seeded into transparent 96-well plate (MTT assay) and allowed to adhere overnight. Lipopeptide solutions of desired concentrations were prepared in cultivation medium. For the cell treatment, the whole volume of the well was replaced with lipopeptide-containing media, incubated for 48 hours and the viability was assessed by MTT test. Briefly, 15 μL of MTT solution (4 mg mL^{-1} in PBS) was added per well and incubated for 4 h in the incubator. The plate was centrifuged (380 × *g*, 10 min), the supernatant was discarded and 200 μL of DMSO was added to the cells to dissolve formazan crystals. The absorbance was measured using a Tecan Sunrise reader at 590/640 nm. The viability was calculated as a ratio between absorbance of treated, control wells, and expressed in percent. To study the time needed to manifest the effect of compound **1** and **2**, the recovery experiments were performed. 20×10^3 cells per well (200 μL) were seeded in a 96-well transparent plate and allowed to adhere overnight. The cells were treated as stated above with 3 μM, 5 μM and 10 μM PUW F or MIN A and mixed multiple times by pipette. At defined time points (1–8 h), the lipopeptide-(exposure)-medium was exchanged for lipopeptide-free medium and the cells were further incubated for 48 hours. The MTT test was performed to check the viability and recovery of the cells.

Assessment of cellular morphology using light microscopy

Live cell imaging was carried out using an Axio Observer Inverted Microscope Z.1. (ZEISS) equipped with an incubation chamber supplied with 5% CO_2. HeLa cells grown in RPMI (Biowest) were seeded at 5×10^3 cells (100 μL) per well into a black 96-well A/2 poly-D-lysine-coated high content imaging plate with an 0.2 mm glass bottom (Corning® BioCoat™). The following day cells were treated, as described above, with different concentrations (20 μM, 5 μM, or 1.25 μM – final volume 100 μL per well) of **1** and **2**. Images were acquired after 48 h of treatment with **1** and **2** using a 100× Plan-Apochromat/1.40 Oil DIC M27 objective and camera adapter 0.63×.

Assessment of membrane damage caused by PUW F and MIN A

HeLa cells in densities of 1×10^4 were seeded on black 96-well plates. The cells were assessed at desired time points (30 min, 45 min, 1, 2, 3, and 6 h) after compound treatments and assessed for LDH-leakage using the CytoTOX One homogeneous membrane integrity assay (Promega) according to the protocol provided by the manufacturer. The provided lysis solution was used to generate maximum LDH leakage. The fluorescence ($560_{Ex}/590_{Em}$) obtained after the compound treatment were related to the maximum LDH leakage and expressed in percent.

HPLC-HRMS determination of PUW F and MIN A concentrations in HeLa cells

To determine the concentration of PUW/MIN in the cell during time 6×10^6 cells were seeded in 6-well plates in 6 mL media and let to adhere overnight. The cells were treated with the compounds at 0.5 and 5 μM concentrations. At the desired time points (5 min, 30 min, 2 h, and 6 h), the cells were harvested by trypsinization and pelleted in 15 mL falcon tubes, subsequently the cells were extracted using 2 mL of 60% ACN aq. containing 1.5% sodium cholate and centrifuged. The resulting samples were analyzed using HPLC-HRMS analysis described above and the concentration was calculated based on the external calibration curve of the pure **1** and **2** and the resulting concentration was expressed as Ag/cell.

Membrane permeabilization assay

Yeast cells (*Saccharomyces cerevisiae* P23) were grown aerobically in YEPG nutrient medium (yeast extract 5 g and peptone 10 g from Oxoid, glucose 20 g in 1 L of water) at 30 °C to mid log phase (OD_{450} nm ~0.5). Cells were harvested, washed, and resuspended (final OD_{450} nm ~0.2) in a citrate–phosphate buffer (0.15 M, pH = 6.0) containing 0.5% glucose and 10 μM propidium iodide (PI, Invitrogen). The tested compounds at final concentrations of 1, 5, and 10 μM were added to 0.2 mL of yeast suspension in a 96-well plate. Membrane permeabilization, as estimated by PI uptake into cells, was monitored as an increase in fluorescence intensity (excitation at 515 nm, emission at 620 nm with bandpass 5 and 10 nm, respectively) at 25 °C using FluoroMax-3 (Jobin Yvon, Horriba) spectrofluorometer with a MicroMax-384 accessory. We used optical filters (3RD500-530 and 3RD570LP, omega optical filters) for the suppression of light scattered by the cells. Ten μM melittin (Sigma) was added to the well as a positive control for cell permeabilization, whereas the buffer addition served as a baseline negative control. The presented data are the recorded intensities without background subtraction.

Lipid bilayer experiments

Black lipid bilayer membranes were formed by painting a solution of 3% (w/v) DOPC/DOPE 2 : 1 (w/w, 1,2-dioleoyl-*sn-glycero*-3-phosphocholine, 1,2-dioleoyl-*sn-glycero*-3-phosphoethanolamine, Avanti lipids) in *n*-decane/butanol (9 : 1, v/v) across a circular aperture (0.5 mm in diameter) separating two compartments of a Teflon chamber. Both compartments contained 2 mL of 10 mM Tris, 1 M KCl, pH 7.4. The temperature was kept at 25 °C. Tested compound were added to the *cis* side of the membrane. The membrane current was measured with Ag/AgCl electrodes (applied voltage 50 mV, *cis* positive), amplified by LCA-200-100G or LCA-4k-1G amplifier (femto), and digitized by a KPCI-3108 card (Keithley). The signal was processed by QuB software.[32]

Antifungal activity

Antifungal activity was evaluated against *Candida friedrickii* (BCC020_2879), *Aspergillus fumigatus* (BCC020_2845), *Fusarium oxysporum* (BCC020_2866), *Trichoderma harzianum* (BCC020_0606), *Bipolaris sorokiniana* (BCC020_1571), *Monographella cucumerina* (BCC020_2872), *Chaetomium globosum* (BCC020_2527), and *Alternaria alternata* (BCC020_0609) using the broth two-fold microdilution method following the standard protocol of broth two-fold microdilution method (CLSI M100-S20).[33] In brief, for the broth microdilution method, the compounds (**1–5d**) were serially diluted at concentrations ranging from 75 to 0.036 μM in a Mueller Hinton broth with 2% glucose in 96-well plates. The inoculum (approximately 5×10^5 CFU mL^{-1} as final concentration) was prepared from an overnight culture and was added to each well containing the compounds. Culture broth (0.1 mL) was added to each well containing compounds. Plates were incubated aerobically at 30 °C for 48 h. Negative controls were prepared using culture media with 50% DMSO in methanol (the dissolving solvent). Fluconazole (32 to 0.0625 μg mL^{-1}) was used as the positive control for all the fungal isolates tested. After incubation, the well with the lowest concentration of the fraction/compound showing some inhibition in growth was taken as the MIC value for the respective organisms. All the experiments were done in triplicate.

3. Results

Cytotoxicity and antifungal properties evaluation of PUW F and MIN A

We initially compared minutissamide A (MIN A, **1**) and puwainaphycin F (PUW F, **2**) to assess the effect of FA length on cytotoxic and antifungal activity. Both lipopeptides possess identical FA functionalization in the proximity of the peptide cycle with a α-carbon substituted by a hydroxyl group, a β-carbon occupied by an amine group engaged in the peptide bond formation with the Pro of the peptide cycle, and a γ-carbon bearing a methyl group. No further FA substitution was observed in **1** and **2** with FA lengths of 12 or 14 carbons, respectively. Both compounds exhibited almost identical IC_{50} values against human HeLa cells as assessed by the MTT assay (Fig. 2A). The IC_{50} values were calculated as 2.8 ± 0.5 μM for **1** and 3.2 ± 0.5 μM for **2** (Fig. 2A). However, **2** exhibited a stronger effect at higher concentrations (5–20 μM), which reduced cell viability by 90–95%, while 70% inhibition was reached after exposure to **1** at this concentration range (Fig. 2A).

We studied the time progression of the cytotoxic effect of the tested compounds using recovery experiments at three concentrations (3, 5 and 10 μM) and evaluated cell viability by MTT, in order to better characterize the differences in the cytotoxic effect of these compounds. A rapid toxic effect on the cell population was observed at concentrations 5 and 10 μM of **2**, with no apparent recovery in cellular viability (after 48 h cultivation), even for the shortest exposure time tested (1 h). The same concentrations of **1** were easily tolerated by the cells for the first two hours, since their viability was comparable to that of the control, after the compound-washout and recovery period (Fig. 2B). Membrane damage, as measured by the lactate dehydrogenase (LDH) leakage, was more profound in **2** compared to **1** in accordance with the recovery experiment. The onset of extracellular LDH leakage was immediate and reached a maximum (60% of released LDH) 2 h after exposure (Fig. 2C) for compound **2** (Fig. 2C). No LDH leakage was recorded for compound **1** at early time points up to 2 h, and LDH started to accumulate in the medium (up to 30% of positive control) only after 3 h suggesting a greater degree of membrane damage (Fig. 2C). The cellular morphology was clearly affected by both **1** and **2** showing apparent cell shrinkage and membrane rupture after 48 h of exposure in concentrations ranging from 2.5 to 20 μM (Fig. 3, S1 and S2†).

We further estimated cellular PUW/MIN concentrations using HPLC-HRMS measurements (Fig. 2D). Compound **2** demonstrated a rapid entry into the cell resulting in a 3–10 times higher cellular concentration compared to **1** at the initial time points (5 to 30 min). The cellular concentration of **1** started to increase after 2 h when it reached a concentration comparable to that of **2** at the initial time points. Interestingly, even the two-fold higher concentration of **1** in the cell compared to **2** was detected at later time points (Fig. 2D). These data correlate well with the delayed cytotoxic effect of **1** as well as the LDH leakage.

The PUWs/MINs also differed substantially in their pore-forming activity as measured in planar DOPC/DOPE membranes. While **2** was able to induce membrane permeabilization at 5 μM concentration, **1** was almost completely inactive under the same conditions. At higher doses both lipopeptides induced detectable increases in membrane current but at considerably different scales (Fig. 4). The typical transmembrane electrical currents were about 10 pA for **1** and 500 pA for **2**, at 10 μM. Due to a great variability in individual pore events, it was not possible to characterize the PUW/MIN at the single-molecule level.

In general, the differences in cytotoxic activity were mirrored in antifungal activity as **2** exhibited substantially higher antifungal potency compared to **1**. We also observed a higher membrane permeabilization activity for **2** compared to **1** in *Candida glabrata* (data not shown) and *Saccharomyces cerevisiae* (Fig. 5) as followed by propidium iodide (PI) entry into cells. Compound **2** induced concentration dependent PI entry into the yeast cells within a few mins at 5 and 10 μM, comparable to

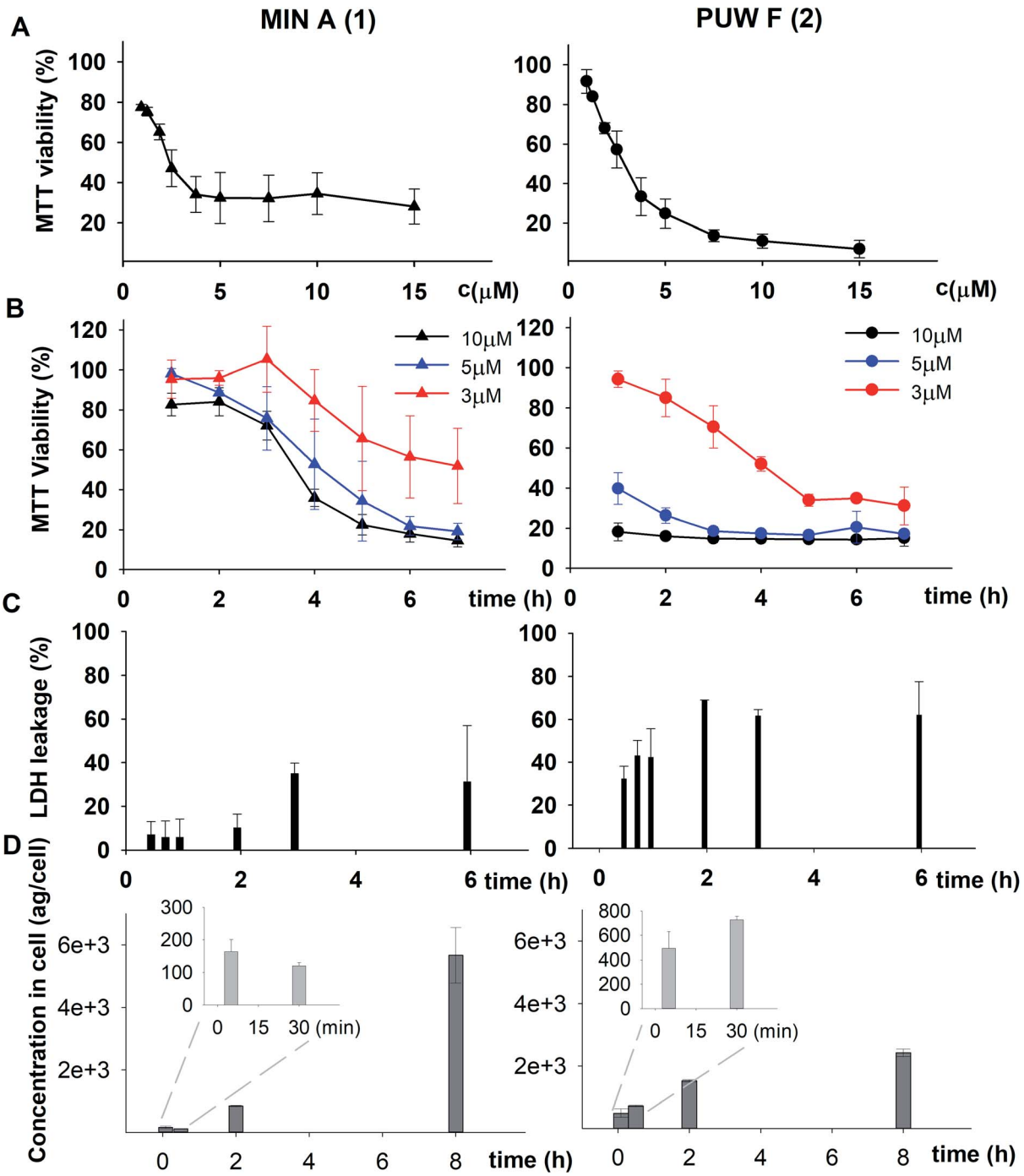

Fig. 2 Comparison of the cytotoxic activity of **1** and **2**: the dose–response curve of both compounds (after 48 h treatment) shows similar IC_{50} values but a stronger effect of **2** at higher concentrations (A). (B) Results of the recovery experiment (treatment followed by 48 h recovery) show more rapid effect on cell viability in **2**. (C) Membrane damage, as assessed by lactate dehydrogenase (LDH) leakage, shows the more potent effect of **2**. (D) Accumulation of **1** and **2** in the cell as assessed using HPLC-HRMS shows the faster entry of **2** in the cell.

the positive control melittin displaying a similar final fluorescence intensity. No membrane disruption was detectable under the same conditions for compound **1**. We tested both compounds for their activity against *Candida* strains and a small panel of filamentous fungi. Compound **2** exhibited a 3 to 129 times lower MIC values compared to **1** with the plant pathogen *A. alternata* and the facultative human pathogen *A. fumigatus* showing the highest sensitivity to both compounds (Table 1).

Preparation of PUW/MIN semi-synthetic variants

We prepared semi-synthetic variants with modified FA moieties based on the preliminary data obtained for compounds **1** and **2** showing that the length of the FA moiety affects both cytotoxicity

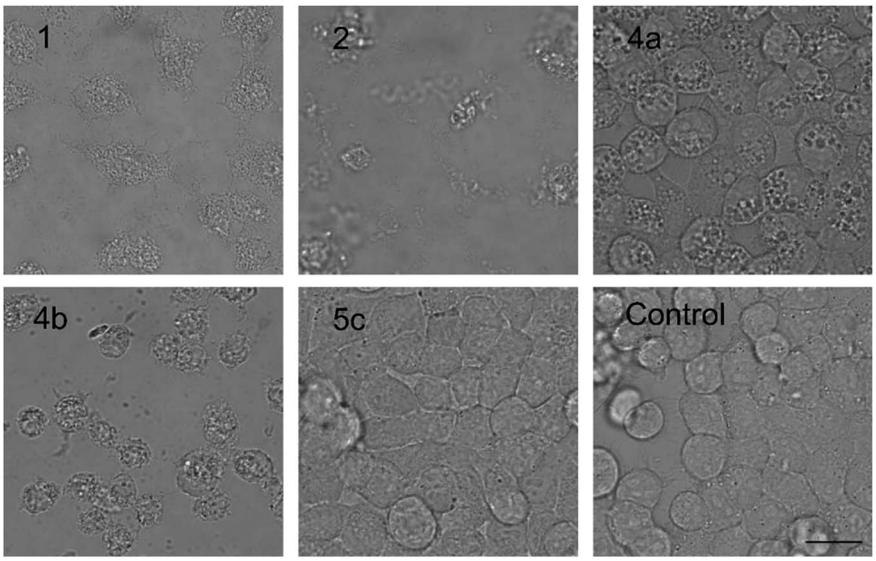

Fig. 3 The morphology of HeLa cells treated with 20 μM compounds under study. Semi-synthetic compound **4b** induced at this concentration clear membrane rupture comparable to natural compounds **1** and **2**. Under treatment of **4a**, the cells appeared stressed but with no membrane rupture at the end of the experiments. No morphology alteration was observed for any of the esterified variants **5a–d** (the figure shows an example morphology for **5c**). For morphological alteration observed at lower concentrations see Fig. S2.† The scale bar represents 20 μm.

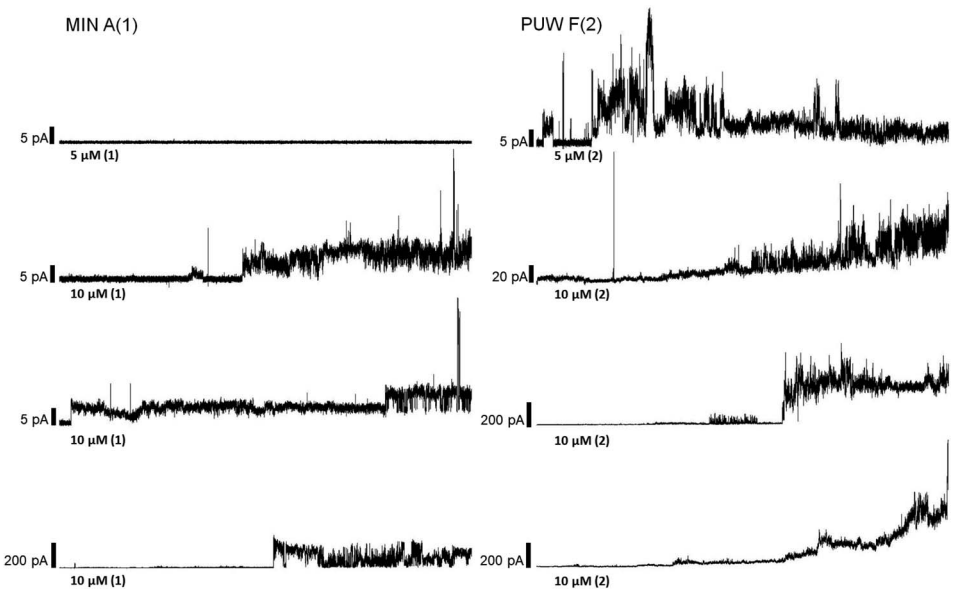

Fig. 4 Pore formation by compounds **1** and **2**. Typical ion current recordings at 5 and 10 μM treatment of **1** and **2** under 50 mV membrane voltage. The membrane was formed from DOPC/DOPE 2 : 1 (w/w) in *n*-decane/butanol (9 : 1, v/v), in a buffer containing 10 mM Tris, 1 M KCl, pH 7.4. Each current trace represents 120 s of recording. Note the different current scale for individual recordings.

and antifungal activity. We used minutissamide C (MIN C, **3**) bearing the oxo-substitution at the FA tail because the FA moieties of compounds **1** and **2** were not easily accessible to chemical modification (Scheme 1). The Wittig-type reaction, with phosphorus ylides preformed from triphenyl phosphonium salts and *n*-BuLi to allow the extension of the aliphatic chain of compound **3**, was initially tested. However, we observed only a small amount of product, which was formed by the side-reaction of *n*-BuLi with the ketone moiety of **3**. Instead, we sought to increase the chain length using other carbon nucleophiles such as alkylmagnesium halides. Moderate yields of the expected tertiary alcohol products were detectable by HPLC-HRMS analysis using this Grignard-reactant (Scheme 1). Reactions with butyl-, octyl-, and nonylmagnesium bromide allowed successful elongation of the FA moiety at C14 by 4, 8, and 9 carbons, respectively. The reaction with methylmagnesium bromide gave rise to a wide variety of side products and reaction with alkylmagnesium halides longer than C9 did not show conversion to the expected products. We performed

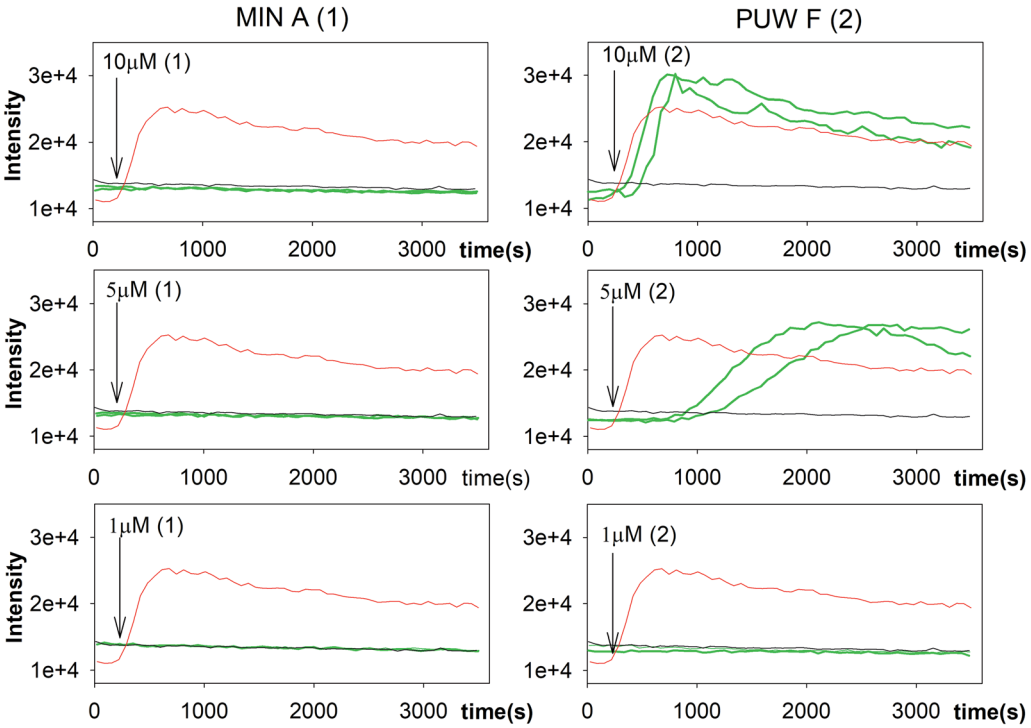

Fig. 5 Membrane permeabilization of *Saccharomyces cerevisiae*. The influx of propidium iodide (PI) across impaired membranes into cells was detected by an increase in PI fluorescence several seconds after the addition of compound **2** but not compound **1**. Green lines represent two sets of experiments; black line and red line represent the negative (buffer solution) and the positive control (melittin), respectively.

Table 1 Antifungal activity of natural and semi-synthetic PUW/MIN variants. The bioactivity of natural reference PUW/MIN variants is highlighted in grey. Abbreviations; NA, no activity at the highest concentration tested (75 μM)

	Natural and semi-synthetic PUW/MIN variants							
	MIC (μM)							
Fungus/compound	**2**	**4a**	**4b**	**1**	**5a**	**5b**	**5c**	**5d**
A. fumigatus	2.34	0.5	3.8	37.5	4.7	9.4	75	37.5
F. oxysporum	75	NA	NA	NA	NA	NA	NA	NA
T. harzianum	37.5	15	NA	NA	75	NA	NA	NA
A. alternata	0.58	0.5	0.1	75	0.6	0.2	0.2	0.2
B. sorokiniana	NA	NA	NA	NA	NA	NA	NA	NA
M. cucumerina	6.25	7.5	30	NA	75	75	37.5	37.5
C. globosum	12.5	60	30	NA	75	75	75	75
C. friedrichii	75	7.5	NA	NA	NA	NA	NA	NA

a subsequent dehydration of the hydroxylated intermediate (Scheme 1) with *p*-TsOH because the formation of a hydroxyl group on the side chain of PUWs/MINs (Scheme 1) can diminish cytotoxicity. Unfortunately, elimination of water only took place at temperatures ≥35 °C resulting in significant decomposition of the compound. We suspected the limitation in time and temperature to be a major reason for the low overall yield of the procedure (1–2% over 2 steps). The elimination of water from the nonyl compound was not feasible before the total decomposition of the molecule. Theoretically, water elimination can occur in three different directions. The non-symmetrical chromatographic peak obtained using HPLC-HRMS indicated the formation of several dehydration products. However, it was not possible to separate these dehydration products and determine which final product was formed preferentially. In Scheme 1, the double bond is drawn tentatively in the direction of the peptide core following Zaitsev's rule. The dehydration of butyl- and octyl-compounds yielded compounds **4a** and **4b**, possessing branched mono-unsaturated FA moieties prolonged at C14 by 4 and 8 carbons, respectively, as confirmed by ^{1}H NMR (Fig. S3 and S4†). The identity of the compounds was validated using HRMS/MS measurements and the specific modified FA-Pro fragments with corresponding mass were obtained for all compounds (Fig. S12 and S13†).

We suspected that hydroxylation might play an important role in bioactivity since the majority of known cyanobacterial cytotoxic lipopeptides contain a hydroxyl group on the FA moiety. Therefore, we attempted to modify the free hydroxyl groups in order to alter the hydrophobicity of the PUW/MIN molecule (namely the α-OH group of FA and –OH substituent at Thr^{8} residues). A Steglich esterification with DMAP and carboxylic anhydrides (Scheme 2) is a mild procedure, which is especially suitable for sterically hindered alcohols.[34] This approach allowed the use of a variety of carboxylic anhydrides with **1** in a convenient one-step procedure with satisfying yields (40–60%). The reactions with acetic, butanoic, hexanoic, and decanoic anhydride led to the formation of double esterified adducts at the α-OH group of the FA moiety and at the OH– in the Thr^{8} resulting in compounds **5a**, **5b**, **5c**, and **5d** (for compound characterization see Fig. S5–S11 and S14–S17†). The

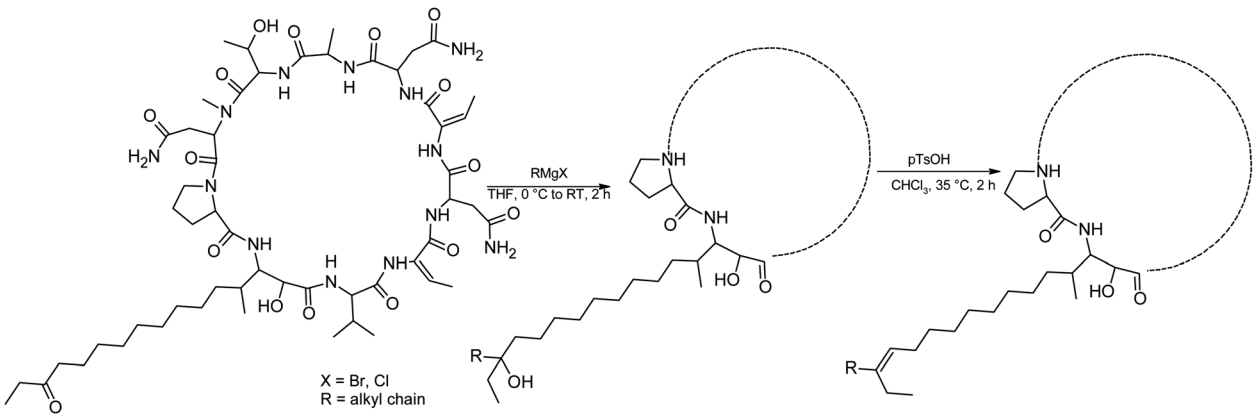

Scheme 1 Grignard-reaction of **3** with alkylmagnesium halides and subsequent dehydration with *p*-TsOH.

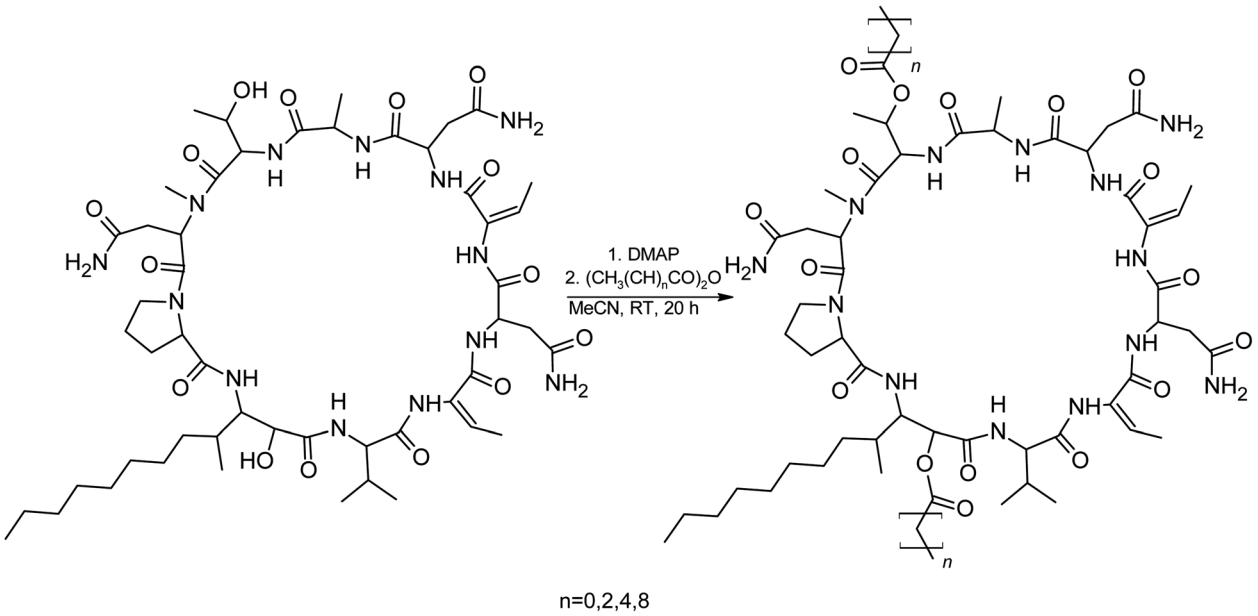

Scheme 2 Steglich esterification of **1** with DMAP and different acid anhydrides.

chromatographic behavior of all products is similar to those observed for **1**, **2**, and **3** (ref. 16) with minor conformational isomer eluting after the major chromatographic peak (Fig. S14–S17†). NMR analyses shows increased shifts of the OH–carbons of the new compounds **5b**, **5c**, and **5d** to 70.89 and 73.36 ppm, for Thr and FA, respectively (exemplary values from substance **3b**), indicating the formation of an ester. Further, the identity of the compounds was in all cases confirmed by the presence of corresponding esterified-FA fragments (Fig. S14–S17†). We did not obtain ^{13}C spectra data due to the high losses observed during the final repurification of **5a**. Instead, we confirmed the structure of the compound using a combination of ^{1}H spectra (Fig. S5†) and HRMS/MS fragmentation (Fig. S14†).

Biological activity of PUW/MIN semi-synthetic variants

The biological activity of semi-synthetic PUW/MIN variants was further evaluated and compared to the bioactivities of the natural PUWs/MINs **1** and **2**. The bioactive properties of **5a–d** were directly compared to compound **1**, used for their preparation. In the case of compounds **4a** and **4b** the original reactant, compound **3**, is oxo-substituted on the FA moiety, while the resulting compounds, **4a** and **4b**, do not contain any heteroatom substitution near the terminal acyl chain and thus these analogs are more similar to compounds **1** and **2**. Accordingly, we selected **2** as a reference compound based on the longer FA moiety of this compound.

The HeLa cells responded to the exposure of compounds **4a** and **4b** in a non-standard manner resulting in a biphasic dose response curve (Fig. 6). Subsequently, it was not possible to calculate the corresponding IC_{50} values. We observed lower viability values at concentration ranges from 0.3–2.5 μM following application of these semi-synthetic variants compared to reference compounds. This was in contrast to the cellular morphology, which appeared normal (Fig. S1 and S2†), with full confluence reached at the end of the experiment. Compound **4a** provided higher viabilities at a higher concentration range

compared to compound **2**. Cells were fully inhibited only at 20 μM of compound **4a**, as also evidenced by cell shrinkage and apparent membrane rupture (Fig. 3). Compound **4b** reached a maximum of 50% inhibition even at a higher concentration range. After treatment with **4b**, the cell morphologies appeared comparable to those in control cells demonstrating no membrane disruption effect. The exception was the highest concentration where a clear cellular rounding and vacuolization was apparent (Fig. 3). Together, this demonstrated an attenuation of the cytotoxic activity of **4a** and **4b** compared to **2**. Consistent with this observation, we recorded membrane rupture, as visualized by microscopy, only at the highest concentrations of compound **4a** while in compound **2** membrane disruption progressed until concentrations of 2.5 μM (Fig. S1†). Surprisingly, cytotoxic activity was almost completely abolished or significantly diminished in treatments with compounds **5a–d** compared to **1** (Fig. 6). While we observed only a weak inhibition at the highest concentration of compounds **5a–c**, compound **5d** showed weak inhibition in the concentration range from 1.2 μM upwards. The cellular morphologies appeared normal across all concentrations (Fig. 3, and S2†) in all the compounds and cells reached full confluence as in the control wells.

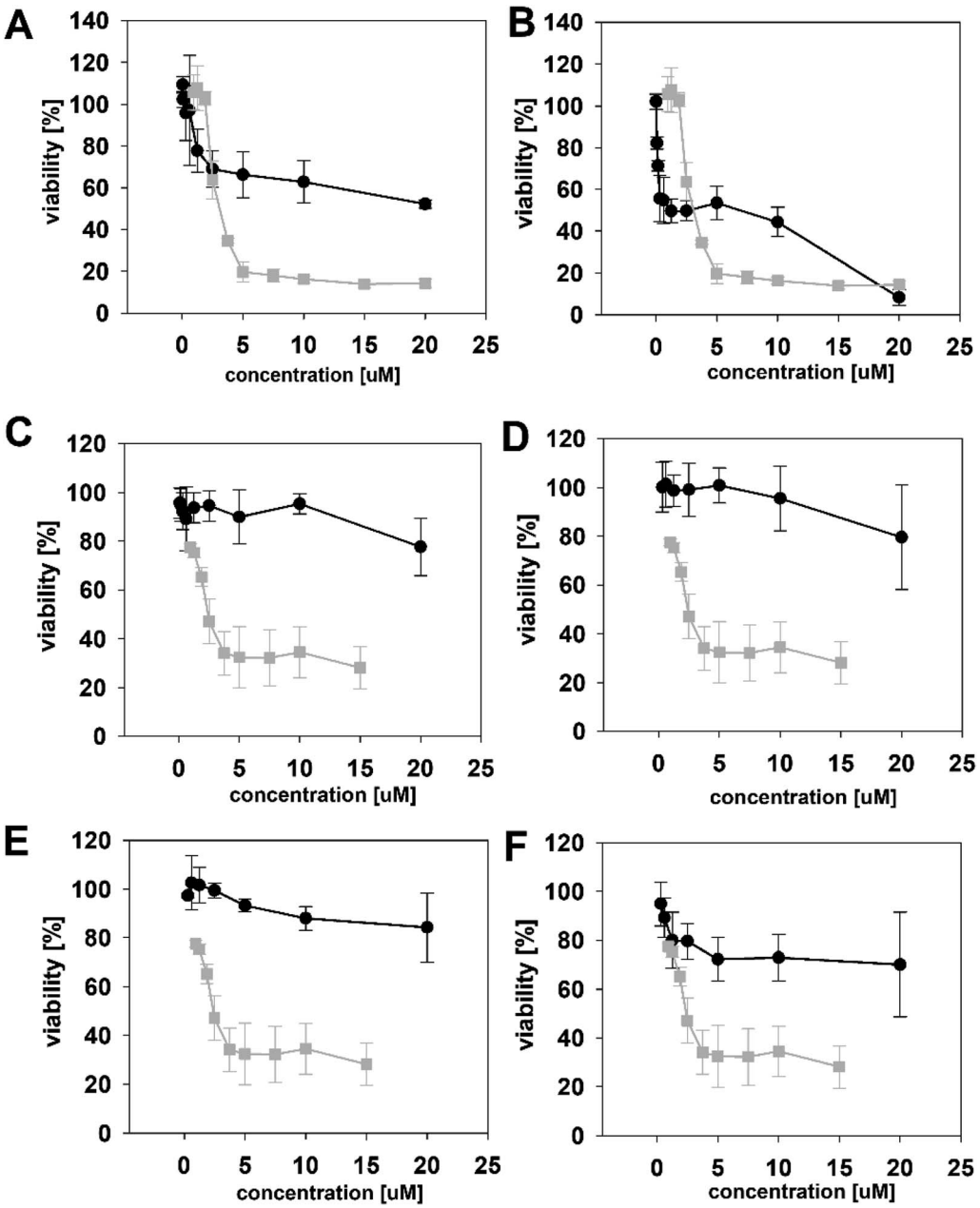

Fig. 6 The dose response curves of the semi-synthetic PUW/MIN variants (black line) in comparison to the reference natural PUW/MIN variant (grey line). Compounds with elongated FA moiety: compound **4a** (A), **4b** (B), and acylated PUW/MIN variants **5a** (C), **5b** (D), **5c** (E), and **5d** (F). Complex dose response curves or low cytotoxic activity prevented calculation of IC_{50} values for semi-synthetic variants in some cases.

The alteration of the FA moiety substantially changed the antifungal properties of PUWs/MINs against most of the fungal strains tested albeit in a species-specific manner. The most profound differences between the natural PUW/MIN variant and the resulting semi-synthetic variants were found in the facultative human pathogen *A. fumigatus* and the plant pathogen *A. alternata*, which showed opposite sensitivities to **4a** and **4b** (Table 1). The FA chain elongation also led to a more profound activity in *T. harzianum* and *C. friedrichii*. The acylated semi-synthetic variants **5a–d** possessed substantially lower MIC values compared to the original compound **1**. We observed an 8 to 375 fold reduction of the MIC values of **4a** and **5a–d** against *A. alternata* and *A. fumigatus*, respectively. However, **5a–d** also caused higher effectivity in *M. cucumerina* and *C. globosum* **5a–d**, resulting in a drop in MIC. These results are notable given the almost complete abolishment of cytotoxic activity in **5a–d**.

4. Discussion

PUWs/MINs are representatives of a relatively large group of cyanobacterial β-amino-FA containing cyclic lipopeptides also comprising muscotoxins,[19,27] trichormamides,[35,36] lobocyclamides,[37] and laxaphycins.[22,23,38] These lipopeptides have biotechnological and pharmaceutical potential.[19,25,39] However, there is limited information available on how FA properties influence antifungal/cytotoxic potency. Natural sources of cyanobacterial cyclic lipopeptides have a restricted range of FA chain lengths, — PUWs/MINs (C10–C18), muscotoxins (C10), and laxaphycins (C8–C10) — which makes direct comparisons difficult. In addition, FA moieties are usually unbranched and FA chains of certain lengths are produced only in modified form (bearing functional groups), such as in PUWs/MINs where the variants with C16 and C18 FA are substituted by oxo or hydroxyl functional groups. Here, we have extended the FA moiety length of PUWs/MINs bearing FA with oxo substitution (compound **3**) by reaction with alkylmagnesium halides and subsequent dehydration using *p*-TsOH. This allowed us to study the effect of PUWs/MINs containing long chain FAs possessing an ethyl side branch and an adjacent double bond (C18 and C22). In addition, we prepared PUW/MIN variants bearing multiple acyl chains by modification of compound **1**. The stereochemistry of compound **1** and **3** was not determined. The stereochemistry of both MIN A and MIN C isolated from *Anabaena minutissima* (UTEX 1613) has previously been described.[17,18] However, in this study both compounds were isolated from different strains and consequently the actual absolute configuration may differ from the published structures. During the chemical modification, no stereogenic center was affected and the modified variants **4a–b** and **5a–d** share a stereochemistry identical to **1** and **3**, respectively. Therefore, the changes in bioactivity can be attributed to the FA modification or lipopeptide acylation.

Our initial results demonstrated that compounds **1** and **2**, differing in the length of their respective FA chains by two methylene groups, manifested similar long-term potency (Fig. 2). However, the application of **2** led to more rapid membrane damage followed by a decrease in the viability of HeLa cells. The actual PUW/MIN concentration within the cell is consistent with these results as the cyclic lipopeptide with a longer FA (**2**) shows more rapid association with the cell compared to **1**. It is notable that compound **1** with a shorter FA chain reached higher cellular concentration in the later time points compared to **2**. However, the cellular concentration of the compound itself does not fully explain its lytic potency. Compound **1** did not cause extensive membrane damage even at concentrations comparable to those of **2** manifesting cell membrane damage. Nevertheless, our results collectively suggest that the FA chain length plays a crucial role in the stability of PUW/MIN-membrane complexes and that even a small difference in the FA chain length affects the onset of the cytotoxic effect to a high degree.

Iturins, and related compounds, with longer FA chains display lower critical micellar concentrations that result in higher antifungal potency.[6] Similarly, compounds **1** and **2** differed in their membrane disruption activity against *Saccharomyces cerevisiae* with **2** promoting membrane disruption while **1** did not. Furthermore, these compounds had differing MIC values against tested fungi with compound **2** being again considerably more potent than compound **1**. Together, these results suggest that the FA chain length of PUWs/MINs plays a more profound role in antifungal activity compared to cytotoxicity. We also observed a similar trend for the semi-synthetic variants **4a** and **4b** with prolonged and branched FA tails. Extension of the FA main aliphatic chain by four (in compound **4a**) and eight carbons (in compound **4b**) led to a substantial decrease in the MIC values against *A. fumigatus* and *A. alternata*, respectively. Although these compounds retained some weak anti-proliferative effect as evidenced by MTT, the cell membrane perturbation was observed at the highest concentration only.

A comparison of natural variants bearing unsubstituted FA (**1** and **2**) with the semi-synthetic analogs **4a** and **4b** containing branched FA (with an ethyl side chain) is not straightforward. However, it is apparent that PUW/MIN variants containing modified FA display an improvement of antifungal activity in a species-specific manner while simultaneously exerting reduced cytotoxic activity. In this study, compounds **1** and **2** containing unsubstituted FA (C12 and C14), exert moderate cytotoxic effects with the resulting IC_{50} values of 2.8 and 3.15 μM. A similar range of IC_{50} was reported for C16 and C18 oxo-substituted FA. However, the semi-synthetic variants **4a** and **4b** possessing unsaturated C18 and C22 with an ethyl side chain do not exert relevant cytotoxicity. Thus, the cytotoxic activity of modified variants is likely diminished by the presence of an ethyl group and adjacent double bond. Neither **1** nor **2** contain double bonds in the exocyclic part of the FA chain. Consequently, the exact position of the unsaturation in compounds **4a** and **4b** is not significant for the presented SAR study as the double bond is newly introduced. For the bioactivity assays, a mixture containing highly enriched tentative isomers following Zaitsev's rule and a minor amount of two other isomers differing in the position of the double bond, was used. It is notable that side methyl FA branching is relatively common in cytotoxic lipopeptides and does not abolish the cytotoxicity against human cells as iturins exhibit cytotoxicity against HeLa

cells with IC_{50} 1.73 μM and 7.8 μM for Iturin A and F_2, respectively.[40] Consequently, it is not the branching itself but rather the length of the side chain that affects the cytotoxic potential. The introduction of the double bond followed by small changes in the 3D structure of the acyl chain should not play a crucial role in the observed decrease of the cytotoxicity as highly potent cytotoxic anabaenolysins contain polyunsaturated FA moiety of a similar length (C18) and exhibit cytotoxicity against HeLa cells with IC_{50} 11 μM.[21] Nevertheless, the FA extension and ethyl branching was accompanied by a species-specific increase of antifungal properties with MIC values of 0.5 μM and 0.1 μM against *A. fumigatus* and *A. alternata* for **4a** and **4b**, respectively.

One of the main achievements of the study is a general improvement of the antifungal activity of PUW/MIN by increasing the hydrophobicity by modification of both the polar hydroxyl groups on Thr and an α –OH on the FA moiety. The double acylation of these functional groups **5a–d** fully diminishes the cytotoxic effect while substantially increasing antifungal activity. Even acylation with C10-mimicking FA tails similar to **1** and **2** abolished cytotoxicity in HeLa cells. Consequently, not only the hydrophobic FA properties but also polar and hydrophilic functional groups are important for the interaction of PUW/MIN with the human cell membrane and its permeabilization. We expect the α-OH on the FA residue to play a crucial role in such interaction as its position after PUW/MIN incorporation into the membrane will allow interaction with the polar phospholipid head. The vast majority of known membrane permeabilizing cyclic lipopeptides including polyunsaturated anabaenolysins[21] or polysubstituted trichormamides,[36] possessed the free α-OH on the FA chain. On the other hand, as apparent from our data, free α-OH is not essential for the antifungal properties of the cyclic lipopeptides. The observed species-specific antifungal properties suggest, that the effect of these modified cyclic lipopeptides (both with extended and branched FA as well as esterified) on the fungi cell is not as general as on the cytoplasmic membrane of human cells and is, moreover, connected to the overall increased hydrophobicity.

5. Conclusions

In the present study we have shown that length of the fatty acid moiety affects the dynamics of the cytotoxic effect in human cells as well the antifungal activity of the naturally occurring cyclic cyanobacterial lipopeptides puwainaphycins and minutissamides. Accordingly, we have modified the lipopeptide fatty acid moiety. In addition, we have acylated the free hydroxyl groups present in the puwainaphycin/minutissamides macrocycle to study their effect on compound bioactivity. Based on the data presented in our study we can conclude that increasing lipopeptide antifungal activity by alternation of hydrophobicity is a feasible way for new fungicides discovery, since the cytotoxicity of these modified variants is strongly diminished. While the prolongation of the FA moiety depends on the presence of a ketone or other functional group(s), the acylation of the hydroxyl group present in the majority of known membrane permeabilizing lipopeptides is an easy way of lipopeptide modification. In this study, we show esterification using DMAP as an effective approach providing satisfying yields.

Conflicts of interest

There are no conflicts to declare.

Acknowledgements

This study was supported by the Ministry of Regional Development of the Czech Republic – EU Interreg ZIEL ETZ Cross-Border cooperation Czech-Bavaria project no. 41. Futher support was grated by the Ministry of Education, Youth and Sports of the Czech Republic, National Programme of Sustainability I, ID: LO1416 and MSCA IF II project (CZ.02.2.69/0.0/0.0/18_070/0010493).

References

1 S. A. Cochrane and J. C. Vederas, *Med. Res. Rev.*, 2016, **36**, 4–31.
2 G. Li, S. Kusari, C. Golz, C. Strohmann and M. Spiteller, *RSC Adv.*, 2016, **6**, 54092–54098.
3 A. Bahadoor, E. K. Brauer, W. Bosnich, D. Schneiderman, A. Johnston, Y. Aubin, B. Blackwell, J. E. Melanson and L. J. Harris, *J. Am. Chem. Soc.*, 2018, **140**, 16783–16791.
4 D. Balleza, A. Alessandrini and M. J. B. Garcia, *J. Membr. Biol.*, 2019, **252**, 131–157.
5 E. Sikorska, M. Dawgul, K. Greber, E. Ilowska, A. Pogorzelska and W. Kamysz, *Biochim. Biophys. Acta, Biomembr.*, 2014, **1838**, 2625–2634.
6 R. Magetdana and F. Peypoux, *Toxicology*, 1994, **87**, 151–174.
7 J. N. Horn, A. Cravens and A. Grossfield, *Biophys. J.*, 2013, **105**, 1612–1623.
8 C. Carrillo, J. A. Teruel, F. J. Aranda and A. Ortiz, *Biochim. Biophys. Acta, Biomembr.*, 2003, **1611**, 91–97.
9 D. Cappelletty and K. Eiselstein-McKitrick, *Pharmacotherapy*, 2007, **27**, 369–388.
10 E. Arrebola, R. Jacobs and L. Korsten, *J. Appl. Microbiol.*, 2010, **108**, 386–395.
11 H. Desmyttere, C. Deweer, J. Muchembled, K. Sahmer, J. Jacquin, F. Coutte and P. Jacques, *Front. Microbiol.*, 2019, **10**, 2327.
12 K. V. Pathak and H. Keharia, *3 Biotech*, 2014, **4**, 283–295.
13 F. Besson, F. Peypoux, G. Michel and L. Delcambe, *J. Antibiot.*, 1979, **32**, 136–140.
14 M. Deleu, J. Lorent, L. Lins, R. Brasseur, N. Braun, K. El Kirat, T. Nylander, Y. F. Dufrene and M. P Mingeot-Leclercq, *Biochim. Biophys. Acta, Biomembr.*, 2013, **1828**, 801–815.
15 P. Urajova, J. Hajek, M. Wahlsten, J. Jokela, T. Galica, D. P. Fewer, A. Kust, E. Zapomelova-Kozlikova, K. Delawska, K. Sivonen, J. Kopecky and P. Hrouzek, *J. Chromatogr. A*, 2016, **1438**, 76–83.
16 J. Mares, J. Hajek, P. Urajova, A. Kust, J. Jokela, K. Saurav, T. Galica, K. Capkova, A. Mattila, E. Haapaniemi, P. Permi, I. Mysterud, O. M. Skulberg, J. Karlsen, D. P. Fewer,

K. Sivonen, H. H. Tonnesen and P. Hrouzek, *Appl. Environ. Microbiol.*, 2019, **85**, e02675-18.
17 H. S. Kang, A. Krunic, Q. Shen, S. M. Swanson and J. Orjala, *J. Nat. Prod.*, 2011, **74**, 1597–1605.
18 H. S. Kang, M. Sturdy, A. Krunic, H. Kim, Q. Shen, S. M. Swanson and J. Orjala, *Bioorg. Med. Chem.*, 2012, **20**, 6134–6143.
19 P. Tomek, P. Hrouzek, M. Kuzma, J. Sykora, R. Fiser, J. Cerny, P. Novak, S. Bartova, P. Simek, M. Hof, D. Kavan and J. Kopecky, *Chem. Res. Toxicol.*, 2015, **28**, 216–224.
20 P. Hrouzek, M. Kuzma, J. Cerny, P. Novak, R. Fiser, P. Simek, A. Lukesova and J. Kopecky, *Chem. Res. Toxicol.*, 2012, **25**, 1203–1211.
21 J. Jokela, L. Oftedal, L. Herfindal, P. Permi, M. Wahlsten, S. O. Doskeland, S. O. and K. Sivonen, *PLoS One*, 2012, **7**, e41222.
22 L. Bornancin, F. Boyaud, Z. Mahiout, I. Bonnard, S. C. Mills, B. Banaigs and N. Inguimbert, *Mar. Drugs*, 2015, **13**, 7285–7300.
23 W. P. Frankmolle, G. Knubel, R. E. Moore and G. M. L. Patterson, *J. Antibiot.*, 1992, **45**, 1458–1466.
24 D. P. Fewer, J. Jokela, L. Heinilä, R. Aesoy, K. Sivonen, T. Galica, P. Hrouzek and L. Herfindal, *Physiol. Plant.*, 2021, 1–12.
25 J. Vestola, T. K. Shishido, J. Jokela, D. P. Fewer, O. Aitio, P. Permi, M. Wahlsten, H. Wang, L. Rouhiainen and K. Svonen, *Proc. Natl. Acad. Sci. U. S. A.*, 2014, **111**, E1909–E1917.
26 W. P. Frankmolle, L. K. Larsen, F. R. Caplan, G. M. L. Patterson, G. Knubel, I. A. Levine and R. E. Moore, *J. Antibiot.*, 1992, **45**, 1451–1457.
27 J. Cheel, J. Hajek, M. Kuzma, K. Saurav, I. Smykalova, E. Ondrackova, P. Urajova, D. L. Vu, K. Faure, J. Kopecky and P. Hrouzek, *Molecules*, 2018, **23**.
28 T. K. Shishido, J. Jokela, C. T. Kolehmainen, D. P. Fewer, M. Wahlsten, H. Wang, L. Rouhiainen, E. Rizzi, G. De Bellis, P. Permi and K. Sivonen, *Proc. Natl. Acad. Sci. U. S. A.*, 2015, **112**, 13669–13674.
29 J. M. Gregson, J. L. Chen, G. M. L. Patterson and R. E. Moore, *Tetrahedron*, 1992, **48**, 3727–3734.
30 J. Mares, J. Hajek, P. Urajova, J. Kopecky and P. Hrouzek, *PLoS One*, 2014, **9**.
31 J. Cheel, P. Urajova, J. Hajek, P. Hrouzek, M. Kuzma, E. Bouju, K. Faure and J. Kopecky, *Anal. Bioanal. Chem.*, 2017, **409**, 917–930.
32 C. Nicolai and F. Sachs, *Biophys. Rev. Lett.*, 2013, **8**, 191–211.
33 K. Saurav, K. Macho, A. Kust, K. Delawska, J. Hajek and P. Hrouzek, *Folia Microbiol.*, 2019, **64**, 645–654.
34 B. Neises and W. Steglich, *Angew. Chem., Int. Ed.*, 1978, **17**, 522–524.
35 S. W. Luo, H. S. Kang, A. Krunic, W. L. Chen, J. L. Yang, J. L. Woodard, J. R. Fuchs, S. H. Cho, S. G. Franzblau, S. M. Swanson and J. Orjala, *Bioorg. Med. Chem.*, 2015, **23**, 3153–3162.
36 S. W. Luo, A. Krunic, H. S. Kang, W. L. Chen, J. L. Woodard, J. R. Fuchs, S. M. Swanson and J. Orjala, *J. Nat. Prod.*, 2014, **77**, 1871–1880.
37 J. B. MacMillan, M. A. Ernst-Russell, J. S. de Ropp and T. F. Molinski, *J. Org. Chem.*, 2002, **67**, 8210–8215.
38 I. Bonnard, M. Rolland, J. M. Salmon, E. Debiton, C. Barthomeuf and B. Banaigs, *J. Med. Chem.*, 2007, **50**, 1266–1279.
39 R. Alvarino, E. Alonso, L. Bornancin, I. Bonnard, N. Inguimbert, B. Banaigs and L. M. Botana, *Mar. Drugs*, 2020, **18**.
40 S. Son, S. K. Ko, M. Jang, J. W. Kim, G. S. Kim, J. K. Lee, E. S. Jeon, Y. Futamura, I. J. Ryoo, J. S. Lee, H. Oh, Y. S. Hong, B. Y. Kim, S. Takahashi, H. Osada, J. H. Jang and J. S. Ahn, *Mar. Drugs*, 2016, **14**.